Biochemical Pharmacology 82 (2011) 1593–1603

Contents lists available at ScienceDirect

Biochemical Pharmacology

journal homepage: www.elsevier.com/locate/biochempharm

H1, a derivative of Tetrandrine, exerts anti-MDR activity by initiating intrinsic apoptosis pathway and inhibiting the activation of Erk1/2 and Akt1/2

Ning Wei [a,*], Geng-Tao Liu [a], Xiao-Guang Chen [a], Qian Liu [a], Feng-Peng Wang [b], Hua Sun [a,*]

[a] Department of Pharmacology, Institute of Materia Medica, Chinese Academy of Medical Sciences and Peking Union Medical College, 1 Xian Nong Tan Street, Beijing, 100050, China
[b] Department of Chemistry of Medicinal Natural Products, West College of Pharmacy, Sichuan University, Ren Min Nan Street17, Chengdu, 610064, China

ARTICLE INFO

Article history:
Received 26 June 2011
Accepted 9 August 2011
Available online 17 August 2011

Keywords:
Drug resistance
Tetrandrine
Anti-cancer
Apoptosis
Survival pathway

ABSTRACT

Currently, multi-drug resistance (MDR) to anticancer drugs is a major obstacle to successful treatment of cancer. Looking for novel compounds with anti-MDR activity is an effectively way to overcome cancer drug resistance. Here, we found that H1, a novel derivate of Tetrandrine, displayed anti-MDR activity *in vitro* and *in vivo*. Average resistant factor of H1 is only 1.6. In KB and KBv200 cancer cells xenograft mice, H1 also displayed favorable anti-MDR activity. It could induce typical apoptosis as indicated by morphologic changes, DNA fragmentation in sensitive and resistant cancer cells. Further studies showed that H1 treatment resulted in the increase of ROS generation, elevation of the Bax/Bcl-2 ratio, loss of mitochondrial transmembrane potential ($\Delta\Psi_m$), release of cytochrome c and AIF from mitochondria into cytosol, and activation of caspase-9 and caspase-3, but had no effect on activation of caspase-8 and the expression of Fas/FasL. On the other hand, H1 also inhibited survival pathways such as the activation of Erk1/2 and Akt1/2. In conclusion, H1 exerts good anti-MDR activity *in vitro* and *in vivo*, its mechanisms may be associated with initiating intrinsic apoptosis pathway and inhibiting the activation of Erk1/2 and Akt1/2. These findings further support the potential of H1 to be used in clinical trial of MDR cancer treatment.

1. Introduction

Cancer multidrug resistant (MDR) modulators could reverse MDR by inhibiting the function of drug transporters and enhancing the sensitivity of resistance cancer cells. In contrast, anti-MDR agents circumvent cancer MDR by directly inhibiting or killing cancer cells with MDR phenotype [1]. The mechanism of MDR was clarified which is important to develop anti-MDR agents. As we all known, numerous mechanisms are contributed to MDR, including alteration at the level of apoptosis sensitivity of cancer cells, abnormal activation of cellular survival signaling pathway, over-expression of drug efflux pumps (such as P-gp), enhanced activity of DNA repair mechanisms, alteration of drug target enzymes, overexpression of enzymes involved in drug detoxification or elimination, and so on [2–4]. However, the imbalance between pro-apoptosis and anti-apoptosis signaling pathway is a key determinant of cancer drug resistance.

Aberrant apoptosis is believed to confer to cancer drug resistance. Apoptosis occurs through two broad pathways: the intrinsic pathway (also known as the mitochondrial pathway) and extrinsic pathway (also known as the death receptor pathway) [5]. Apoptosis via intrinsic pathway can be triggered by anticancer drugs. Bcl-2 family members are determinants of cellular drug sensitivity of many cancers. Increased levels of anti-apoptosis protein such as Bcl-2, or reduced expression of pro-apoptosis members such as Bax is associated with increased resistance of cancer cells to anticancer drugs [6]. In contrast to intrinsic pathway, extrinsic pathway of apoptosis is induced by ligand binding of death receptors. The most important ligand-death receptor is Fas ligand–Fas [7]. Binding of Fas ligand (FasL) to Fas leads to recruitment of FADD (Fas-associated death domain) [8]. The oligomerized receptors and recruited FADD form a complex termed DISC (death-inducing signaling complex), which can bind to initiator caspases such as caspase-8 and -10, thereby triggering the caspase cascades such as activation of caspases-3, -7, and -9, and leading to apoptotic events. The alteration of Fas/FasL and caspase-8 expression level is also believed to confer to cause cancer drug resistance [9–11].

On the other hand, survival signaling pathways including mitogen-activated protein kinase (MAPK) and phosphatidylinositol 3-kinase (PI3K) pathways, which are often constitutively activated in many types of cancer [12,13]. Survival signaling via the epidermal growth factor receptor (EGFR), MAPK, and PI3K pathways is counterbalanced by downstream signaling pathways resulting to apoptosis. However, abnormal activation of the MAPK

* Corresponding authors. Tel.: +86 10 63165178; fax: +86 10 63017757.
E-mail addresses: chinaweining@yahoo.com (N. Wei), sunhua@imm.ac.cn (H. Sun).

0006-2952/$ – see front matter © 2011 Elsevier Inc. All rights reserved.
doi:10.1016/j.bcp.2011.08.012

and PI3K/Akt/mTOR pathway confers resistance to many types of cancer chemotherapy, and is a poor prognostic factor for many types of cancer [14,15].

Tetrandrine (Tet) is a bisbenzylisoquinoline which is the main active component in the root *Stephania tetrandra* S. Moore. Previous studies have shown that Tet could inhibit the proliferation and induce apoptosis of several cancers, including breast cancer, lung cancer, neuroblastoma, hepatoma, leukemia, and so on [16,17]. Its mechanisms are associated with elevated the expression of p53, p21 and Bax, induced the Cdk inhibitor p1, decreased the expression of cyclin D1, increased the release of mitochondrial cytochrome c, activated caspases-3, -8 and -9 [18,19]. All of these results suggested that Tet could induce apoptosis, although the exact mechanism is still uncertain. BrTet and H1 are bromized derivative of Tet, and synthesized by Prof. Feng-Peng Wang. In preliminary screening, BrTet and H1 were shown to be more potent than Tet in reversal MDR *in vitro*. Our group has reported that BrTet and H1 displayed reversal MDR activity [20,21]. At non-cytotoxic concentration, they could inhibit the expression and function of P-gp. Interestingly, we observed that cytotoxic concentration of H1 also exerted anticancer activity against resistant cancer cells. Here, we further evaluate anti-MDR activity of H1 *in vitro* and *in vivo*, and investigate its effect on cellular apoptosis pathways and survival pathways in sensitive and resistant cancer cells.

2. Materials and methods

2.1. Chemicals

H1 was kindly provided by Prof. Feng-Peng Wang (Department of Chemistry of Medicinal Natural Products, West College of Pharmacy, Sichuan University, Chengdu, China). It is a slight yellow powder with 99.0% purity, and freshly solved in dimethyl suifoxide (DMSO, Amresco, Solon, OH, USA) before use. The chemistry structure is shown in Fig. 1A. Molecular formula: $C_{27}H_{40}N_2O_6Br$, molecular weight: 690. Z-LEDH-FMK, a caspase-9 inhibitor, was purchased from BD Biosciences (San Jose, CA, USA). Paclitaxel (Tax), doxorubicin (Dox), vincrinst ine (Vcr), 1-(4,5-dimethylthiazol-2-yl)-3, 5-diphenyformazan (MTT) and other chemicals were purchased from Sigma chemical Co. (St. Louis, MO).

2.2. Cell lines and cell culture

The MDR cell lines KBv200, MCF-7/dox, A549/tax were generously provided by Prof. Xiao-Guang Chen. Other cancer cell lines were kept in our group. All of the cell lines were all grown in RPMI1640 (GIBCO BRL) medium supplemented with 10% heat-inactivated newborn calf serum, 100 U/ml penicillin, and 100 μg/ml streptomycin. To maintain drug resistance, 200 nM Vcr, 500 nM Dox, and 10 nM Tax was added to the culture of KBv200, MCF-7/dox, and A549/tax cells, respectively. All experiments were performed after 7–10 days of incubation in drug-free medium [21].

2.3. Cytotoxicity assay

Cell viability was assessed with MTT assay. In detail, cells were seeded in 96-well multiplates. After an overnight incubation (37 °C with 5% CO_2), various concentrations of H1 was added into wells and incubated for another 72 h. Thereafter, 100 μl of 0.5 μg/ml MTT was added to each well after withdraw the culture medium and incubated for an additional 4 h. The resulting formazan was dissolved in 150 μl DMSO after aspiration of the culture medium. Plates were placed on a plate shaker for 30 min and read immediately at 570 nm using a microplate reader (Bio-Rad Model 450). The IC_{50} was determined in duplicates and each experiment was repeated at least three times under identical conditions. IC_{50} value was defined as the drug concentration that inhibits 50% cell growth compared with the untreated controls and calculated by Graphpad Prism 6.0 software. In addition, the resistant factor of H1 and references is calculated according to the following equation: Resistant factor = IC_{50} (corresponding resistant cells)/IC_{50} (parental cells) [22].

2.4. DAPI staining assay

In brief, KB and KBv200 cells (1×10^5 cells/well) were seeded into 6-well plates and treated with different concentrations of H1 for 24 h. The cells were fixed with 4% paraformaldehyde for 15 min

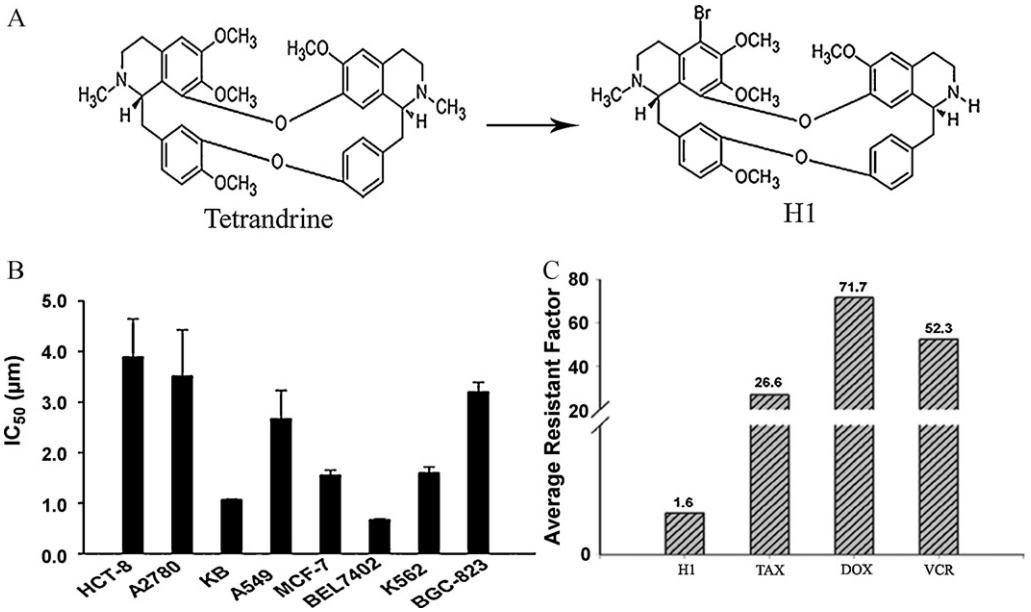

Fig. 1. Anti-MDR activity of H1 *in vitro*. (A) Chemical structures of Tetrandrine and H1; (B) anticancer profile of H1, cytotoxicity of H1 on 8 types of cancer cells were determined by MTT assay as described in Section 2. Data are the means ± SD of at least three independent experiments. (C) Average resistance factor of H1 and references, on the basis of cytotoxic activity of agents against resistant and its parental cancer cells, calculated average factor of H1 and 3 reference agents.

at room temperature. After washed with PBS (phosphate buffered saline), the cells treated with 0.1% triton for 10 min at room temperature. Washed with PBS three times, 2 μl DAPI (5 μg/ml) was added to the cells for 5 min, after which they were examined by fluorescence microscopy. Apoptotic cells were identified by condensation and fragmentation of chromatin.

2.5. DNA fragmentation

After treatment of H1 for 24 h, selective extraction of degraded DNA was performed by using Apoptotic DNA Ladder Kit (Applygen Technologies Inc., China). Subsequently, loading buffer (0.25% bromophenol blue, 0.25% xylene cyanol FF, 30% glycerol) was added. Horizontal gel electrophoresis (1% agarose containing ethidium bromide (0.5 mg/ml)) was performed in Tris–borate–EDTA buffer (TBE, pH 8.0) at 80 V. DNA was visualized under UV light and photographed by Gel Logic Imaging Systems (Kodak Scientific Imaging Systems, CT).

2.6. Annexin V-propidium iodide binding assay

Briefly, following 24 h treatment of H1, KB and KBv200 cells were resuspended with the cold binding buffer. According to the manufacture's instruction (KeyGEN Biotech Inc., China), 5 μl of Annexin V-FITC and 5 μl of propidium iodide (PI) were added and the cells were incubated for 10 min in dark at room temperature. Flow cytometry analysis was performed using a FACS (Beckman Coulter, USA). Annexin V- and PI-double negative cells were defined as live cells. Annexin V-positive, PI-negative cells were defined as early apoptotic cells and Annexin V- and PI-double-positive cells were defined as late-arising apoptotic cells.

2.7. Cell cycle analysis

Following 24 h treatment of H1, the cells were collected, fixed in 70% ice-cold ethanol, and stored at 4 °C overnight. To determine cell cycle distribution, the cells were transferred into PBS, incubated with RNase A (50 μg/ml) for 30 min at 37 °C, followed by 30 min treatment with PI (50 μg/ml) at 37 °C. The cells were washed and resuspended in PBS. The fluorescence levels were analyzed by flow cytometry (Beckman Coulter, USA).

2.8. Mitochondrial transmembrane potential ($\Delta\Psi_m$) measurement

The $\Delta\Psi_m$ was analyzed by JC-1 Mitochondrial Membrane Potential Assay Kit (KeyGEN Biotech Inc., China). JC-1 (5,5′,6,6′-tetra-chloro-1,1′,3,3′-tetra-ethylbenzimidazol-carbocyanine iodide) is capable of selectively entering mitochondria, where it forms aggregates and emits red fluorescence when $\Delta\Psi_m$ is high. At low $\Delta\Psi_m$, JC-1 cannot enter into mitochondria and forms monomers emitting green fluorescence. The ratio between green and red fluorescence provides an estimate of changes in the mitochondria membrane potential ($\Delta\Psi_m$). KB and KBv200 cells were treated with desired concentrations of H1 for 24 h. After trypsinisation and PBS washing, 1×10^5 cells were incubated for 20 min in freshly prepared JC-1(1 mM) solution at 37 °C. Spare dye was removed by dye buffer solution washing. The cell-associated fluorescence was measured with FACS (Beckman Coulter, USA)

2.9. Measurement of ROS generation

The levels of ROS (Reactive Oxygen Species) were measured by DCFH-DA which is a freely permeable tracer specific for ROS. DCFH-DA can be deacetylated by intracellular esterase to the non-fluorescent DCFH which is oxidized by ROS to the fluorescent compound 20, 70-dichloroflorescein (DCF). Thus, the fluorescent intensity of DCF is proportional to the amount of ROS produced by the cells [23]. 1×10^5 cells/well were exposed to H1 for 24 h and 1 mM H_2O_2 used as a positive control. Then, cells were harvested, rinsed twice with PBS and incubated with DCFH-DA (100 μM) in the dark at 37 °C for 30 min. The cells were washed and resuspended in PBS. The cell-associated fluorescence was measured with FACS (Beckman Coulter, USA)

2.10. Western blot analysis

Cells were harvested and rinsed twice with PBS, and lysed in denaturing lysis buffer (Applygen Technologies Inc., China) for 30 min on ice, centrifuged $12000 \times g$ for 15 min at 4 °C. Protein concentrations were determined by BCA assay (Applygen Technologies Inc., China). Equal quantities (40 μg of protein) of cell extract were resolved by 10% SDS-PAGE, the resolved protein were electrophoretically transferred to PVDF membrane, and blocked with 5% fat-free dry milk in TBST for 1.5 h at room temperature. The membrane was immunoblotted with mouse monoclonal antibody to caspase-3 (1:1000), caspase-9 (1;1000), mouse monoclonal antibody to Bax and Bcl-2 (1:500), rabbit polyclonal to Fas and FasL (1:500), mouse monoclonal antibody to cytochrome c (1:1000), rabbit polyclonal to AIF (1:500), rabbit polyclonal to p-Erk and Erk (1:1000), rabbit polyclonal to β-actin (1:2000) (Santa Cruz Biotechnology, Santa Cruz, USA), rabbit polyclonal to active capase-3 (1:1000), rabbit polyclonal to p-Akt and Akt (1:1000) (CST, USA), rabbit polyclonal to capase-8 (1:1000) (Bioworld Technology Inc., China), in 5% milk TBST, at 4 °C overnight. The membranes were washed three times, incubated with HRP-conjugated secondary antibodies for 1.5 h at room temperature, and washed extensively before detection. The membranes were subsequently developed using ECL (Fuji Film, Japan) reagent (Applygen Technologies Inc., China) and exposed to film according to the manufacturer's protocol.

2.11. In vivo efficacy evaluation

KB and KBv200 xenografts were initially established in female BALB/c nude mice (Center of Experimental Animals, Chinese Academy of Medical Sciences) at 6–7 weeks of age and body weight of 18–20 g. The mice were implanted with 1×10^7 parental KB or 1×10^8 resistant KBv200 cells, respectively, by subcutaneous injection into the interscapular area. Xenografts were maintained for two generations by subcutaneous implantation of about 50 mg non-necrotic tumor tissue using a trocar [20]. Length and width of tumors were measured, and the tumor volume (mm^3) was calculated by the formula, $\pi/6 \times L \times W^2$, where length ($L$) and width ($W$) were determined in mm. Drug treatment was started when the tumor size reached to above 100 mm^3. The nude mice with xenografts were divided into groups randomly. Each group contained 6 mice and was treated with various regimens on day 1. A dose of 0.4 mg/kg Vcr was administered on day 1 after grouping the mice and then every other day for one time, this group used as positive control. A group of nude mice was only treated with sterile normal saline as normal control. Three dosages of 10, 15 and 20 mg/kg H1 dissolved in sterile normal saline were given from day 1, once daily for 14 days. All agents were injected intraperitoneally (ip) in a volume of 0.2 ml/20 g body weight. Evidence of drug effect is described by the following parameters: $\%T/C$ = [Δtumor volume of treated group]/[Δtumor volume of control group] × 100%. By National Cancer Institute criteria, agents which confer $\%T/C$ less than 40% are considered to be minimally active, and $\%T/C$ less than 10% are considered to be highly active [24]. The curve of tumor growth was drawn according to relative tumor volume and treatment time. In addition, tumors were excised from the mice and weighted it. The rate of inhibition (IR) was calculated

Table 1
Cytotoxicity of H1 and reference drugs against pairs of resistant and sensitive cell lines.

	IC_{50}(μM)					
	KB	KBv200	MCF-7	MCF-7/dox	A549	A549/tax
H1	1.568 ± 0.017	1.963 ± 0.287	1.556 ± 0.101	3.139 ± 0.059	2.669 ± 0.561	2.626 ± 0.090
TAX	0.040 ± 0.011	0.897 ± 0.283	0.013 ± 0.011	0.429 ± 0.132	0.010 ± 0.007	0.245 ± 0.055
DOX	0.021 ± 0.020	1.087 ± 0.149	0.075 ± 0.012	11.588 ± 1.087	0.049 ± 0.010	0.432 ± 0.194
VCR	0.029 ± 0.006	1.334 ± 0.166	0.055 ± 0.008	4.662 ± 0.581	0.208 ± 0.058	5.439 ± 0.998

Data are means ± SD of at least three independent experiments.

according to the formula: IR (%) = 1 − (mean tumor weight of the experimental group/Mean tumor weight of the control group) × 100%.

2.12. Statistical analysis

Data were expressed as means ± SD. Statistical analysis of the data was performed using the one-way ANOVA. $P < 0.05$ was considered statistically significant.

3. Results

3.1. Anticancer activity of H1 in human tumor cell lines

Firstly, we determined the cytotoxic activity of H1 against 8 types of human cancer cells including HCT-8, A2780, KB, A549, MCF-7, Bel7402, K562, BGC-823. The results shown in Fig. 1B, H1 displayed potent cytotoxicity against 8 types of human cancer cells with a mean IC_{50} of 2.272 μM. KB and Bel7402 cells displayed higher susceptibility with the IC_{50} values of 1.068 and 0.671 μM, respectively. In contrast, HCT-8 cells exhibited the lowest susceptibility to H1 with the IC_{50} value of 3.890 μM.

3.2. H1 displays potent anti-MDR activity in MDR cell lines

Subsequently, we tested whether H1 had anti-MDR activity by using three MDR sublines KBv200, A549/tax and MCF-7/dox. Drug-sensitive parental KB, A549 and MCF-7 cell lines and anticancer drugs including Vcr, Tax and Dox were used as references. As shown in Table 1, H1 displayed significant cytotoxicity in the KBv200 subline examined, with an IC_{50} value of 1.963 μM. Notably, the resistance factor of H1 on KBv200 cells was only 1.8, which was much lower than that of the reference drug Dox (RF = 51.7), Vcr (RF = 46.0), and Tax (RF = 22.4). The cytotoxicity of H1 was also potent to the MCF-7/dox subline (IC_{50} = 3.139 μM), while the IC_{50} against the parental cells was 1.556 μM. Nevertheless, it was still much more potent than the positive drug Dox (RF = 154.5), Vcr (RF = 84.8), Tax (RF = 33.0). The IC_{50} of H1 in A549/tax cells similar to that of the parental cell lines. Based on the above results, we calculated the average resistant factor of H1 and references. The average RF of H1 was only 1.6, while that of Dox, Vcr and Tax were 71.7, 52.3 and 26.6, respectively (Fig. 1C). Thus, H1 displayed good anti-MDR activity *in vitro*.

3.3. Anti-MDR activity of H1 in vivo

We further evaluate anti-MDR activity of H1 *in vivo* by established KB and KBv200 xenograft models. The results are shown in Table 2 and Fig. 2, Vcr group displayed good anticancer effect on KB xenograft model, its %*T*/*C* and inhibitory rate of tumor weight were 15.65% and 82.1%, respectively. But the %*T*/*C* and inhibitory rate of tumor weight of Vcr group were only 87.71%, 27.7% in KBv200 xenograft. Thus, it suggests that we have successfully established KBv200 resistant model for evaluating anti-MDR activity of H1. In KB xenograft model, H1 (20 mg/kg) exhibited good anticancer activity, and the %*T*/*C* and inhibitory rate of tumor weight were 22.4% and 79.0%. Inspiringly, in KBv200 xenograft model, H1 also have significant anticancer activity, and the %*T*/*C* and inhibitory rate of tumor weight were 30.3% and 74.9%, respectively. Notably, H1 also displayed favorable anti-MDR activity *in vivo*.

3.4. H1 has not affect cell cycle distribution of KB and KBv200

Cell cycle distribution of KB and KBv200 cells was determined by flow cytometric analysis. As shown in Fig. 3A, treatment of H1 for 24 h did not alter the cell cycle distribution of KB and KBv200 cells. S phase has not decreased significantly. Moreover, we

Table 2
Inhibition effect of H1 on tumor growth of KB and KBv200 xenograft nude mice.

	Group	Mice number (initial/end)		Body weight initial/end)		Tumor weight g)	Inhibition rate (%)
KB	Control	6	6	18.3 ± 0.2	21.5 ± 0.4	1.31 ± 0.29	–
	H1 10 mg/kg	6	6	18.4 ± 0.3	21.4 ± 0.3	0.87 ± 0.28*	33.7
	H1 15 mg/kg	6	6	18.4 ± 0.2	20.9 ± 0.3	0.43 ± 0.19**	67.1
	H1 20 mg/kg	6	6	18.4 ± 0.2	18.6 ± 0.5	0.28 ± 0.15***	79.0
	Vcr	6	6	18.6 ± 0.3	21.3 ± 0.3	0.24 ± 0.13***	82.1
KBv200	Control	6	6	20.9 ± 0.5	23.4 ± 0.4	1.79 ± 0.23	–
	H1 10 mg/kg	6	6	20.9 ± 0.3	23.8 ± 0.5	1.32 ± 0.34*	26.5
	H1 15 mg/kg	6	6	20.8 ± 0.3	21.9 ± 0.4	0.88 ± 0.10**	50.9
	H1 20 mg/kg	6	6	21.0 ± 0.4	20.8 ± 0.5	0.45 ± 0.17**,*	74.9
	Vcr	6	6	20.6 ± 0.3	22.2 ± 0.4	1.29 ± 0.27*	27.7

The experiment was carried out using nude mice implanted subcutaneously (sc) with KB (1×10^7/0.2 ml) or KBv200 (1×10^8/0.2 ml) cells under the right armpits. Animals were randomized into five groups including control, Vcr and three desired dosages of H1, ip, qd × 15. At the end of the experiment, body weight and tumor tissue were weighted. Data are means ± SD of the tumor weight for each group of 6 experimental animals.

* $P < 0.05$ *vs.* control group.
** $P < 0.01$ *vs.* control group.
*** $P < 0.001$ *vs.* control group.

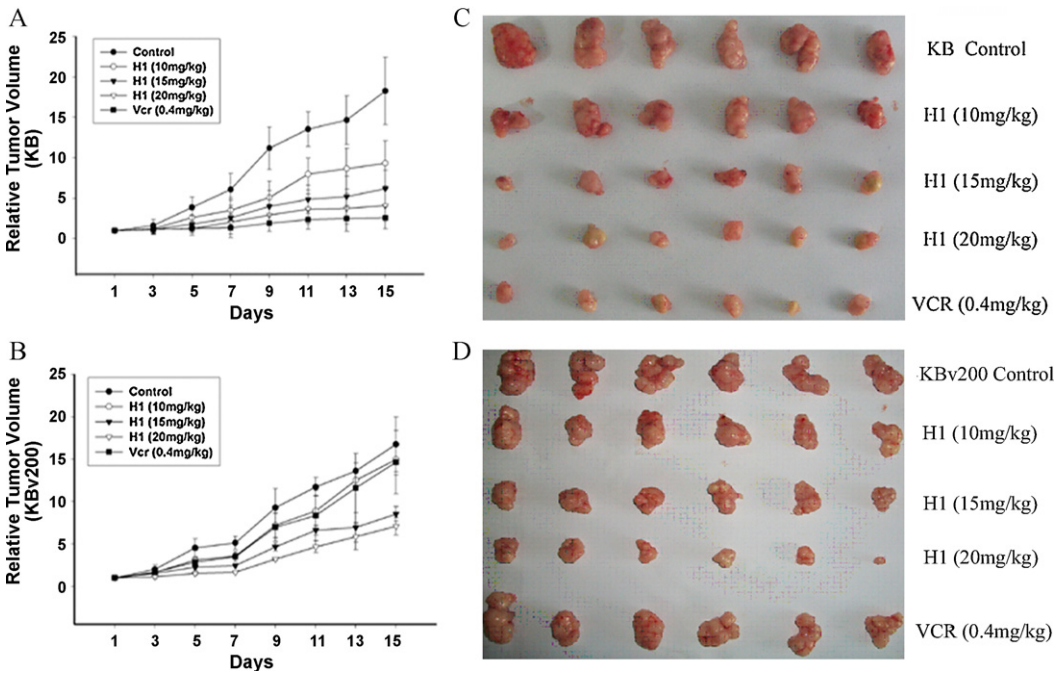

Fig. 2. Anti-MDR activity of H1 *in vivo*. (A and B) The experiment was carried out using nude mice implanted subcutaneously (sc) with KB (1×10^7/0.2 ml) or KBv200 (1×10^8/0.2 ml) cells under the right armpits. Animals were randomized into five groups including control, Vcr and three desired dosages of H1, ip, qd × 15. Tumor growth was monitored staring on the first day of treatment and the volume of the xenograft was measured every 2 days. Data are means ± SD of the relative tumor volume for each group of 6 experimental animals. (C and D) The picture showed the tumor size of KB and KBv200 xenograft at the end of the experiment.

observed the increase of sub-G1 phase with the concentration of H1. It suggests that H1 could induce apoptosis of KB and KBv200 cells.

3.5. H1 induces apoptosis of KB and KBv200 cells

Apoptosis has been determined to be responsive to H1-mediated anticancer activities. Accordingly, we investigated the ability of H1-induced apoptosis of KB and KBv200 cells by using DAPI staining, internucleosomal DNA fragmentation, and flow cytometric analysis.

Firstly, we focused on the morphological changes of apoptosis induced by H1. As shown in Fig. 3B, KB and KBv200 cells with normal morphology were observed in control group, whereas KB and KBv200 cells with fragmented chromatin and apoptotic bodies were noted following treatment with H1. However, KB cells exhibited slight susceptibility to induce apoptosis than KBv200 cells. These results suggest that H1 is capable of inducing marked apoptotic morphological changes in KB and KBv200 cells.

Subsequently, we examined the internucleosomal DNA fragmentation at various concentrations of H1. We found that treatment with H1 at concentrations ranging from 8 μM to 12 μM for 24 h caused classic internucleosomal DNA fragmentation. As the result shown in Fig. 3C, H1 at a concentration of 8 μM initiated the DNA ladder fragmentation.

To further quantify apoptotic cells induced by H1 using Annexin V-propidium iodide binding assay. As the results shown in Fig. 3D, H1 could induce apoptosis of KB cells and KBv200 cells with good concentration-dependent manner. In addition, apoptosis potency of H1 in KB cells is a little more than that of KBv200 cells (Fig. 3E and F). This result is concordant with the anti-MDR activity *in vitro*.

3.6. H1-induced apoptosis is dependent on the activation of caspase-9 and -3

Apoptosis is characterized by a well-organized sequence of cellular events, resulting in the activation of the caspase cascades. Caspase-9 is the main caspases member mediated intrinsic apopstosis, while caspase-3 is one of the key effector caspases in downstream execution apoptotic pathway. Thus, we detected the activation of caspase-9 and caspase-3. As shown in Fig. 4A, the activity of caspase-9 and -3 was significantly enhanced after the treatment of H1. To further confirm whether treatment with H1 induces caspase-9 dependent apoptosis, the cells were treated with a cell-permeable caspase-9 inhibitor, Z-LEHD-FMK (20 mM) before addition of H1. As shown in Fig. 4B, treatment with Z-LEHD-FMK significantly reduced the ability of H1-induced apoptosis of KB and KBv200 cells. These results suggest that H1-induced apoptosis is mediated through a caspase-9 dependent signaling cascade.

3.7. H1-induced apoptosis is not through death receptor pathway

Fas is the well-known member of the TNF receptors superfamily, which activates apoptosis by recruiting a number of adaptor, signaling, and effector proteins. Expression of Fas receptor and its respective ligand FasL were detected by Western blot. As shown in Fig. 4C, treatment with H1 for 24 h did not affect the expression of Fas and FasL in KB and KBv200 cells. Caspase-8 is the crucial initiator caspases in signal transmission by death receptor pathway. The activation of caspase-8 was analyzed by Western blot. As shown in Fig. 4C, the zymogen of pro-caspase-8 did not change either in sensitive or resistant cells. These results suggest that the apoptosis induced by H1 was not through the Fas/FasL mediated extrinsic pathway in KB and KBv200 cells.

3.8. H1 initiates release of cytochrome c, AIF, loss of $\Delta\Psi_m$ and elevates the ratio of Bax/Bcl-2

The collapse of the mitochondrial membrane potential is an early step in the induction of apoptosis by the mitochondrial pathway. Therefore, the variation of mitochondrial membrane potential was determined by JC-1 staining analysis in KB and KBv200 cells. In non-apoptotic cells the dye accumulates and

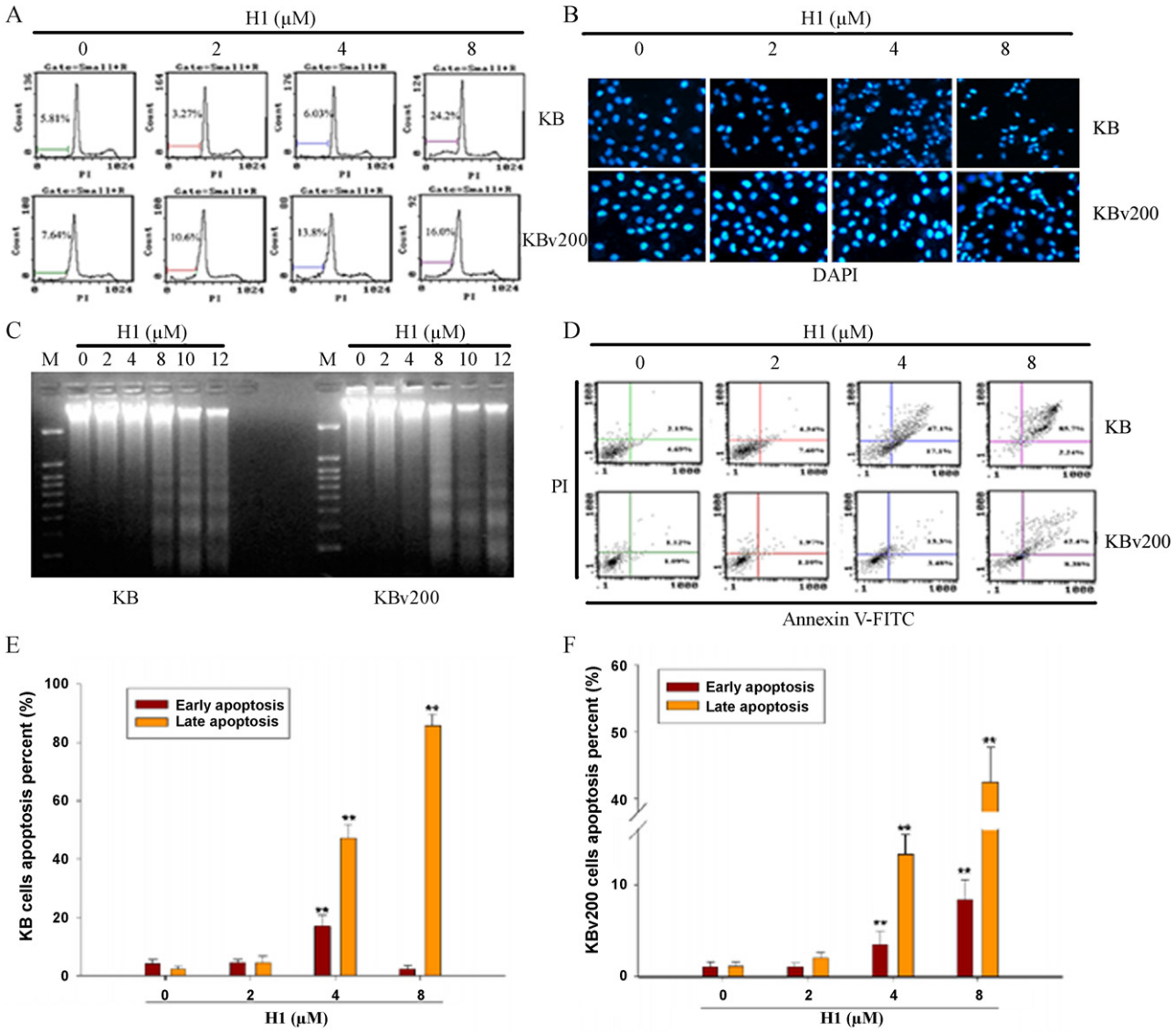

Fig. 3. Apoptosis of KB and KBv200 cells induced by H1. (A) Effect of H1 on the cell cycle distribution. KB and KBv200 cells treated with or without H1 for 24 h, then the cells harvested, fixed and stained with propidium iodide for flow cytometric analysis. The percentage of cells with hypodiploid DNA content (sub-G1) represents fractions undergoing apoptotic DNA fragmentation. The results are representative of three independent experiments. (B) Apoptosis of KB and KBv200 cells detected by DAPI staining. KB and KBv200 cells treated with or without H1 for 24 h, then the cells harvested, fixed and stained with 4′,6-diamidino-2-phenylindole. (C) Apoptosis of KB and KBv200 cells detected by DNA Ladder analysis. KB and KBv200 cells treated with or without H1 for 24 h. DNA was extracted from the harvested cells, DNA fragmentation was detected by agarose gel elcetrophoresis and photographed by Gel Logic Imaging Systems. (D) Apoptosis of KB and KBv200 cells detected by PI-Annexin V-FITC binding assay. Cells treated with or without H1 for 24 h at indicated concentrations, stained with Annexin V and PI before subjecting into FACScan for analysis. Lower right part (Annexin V^+/PI^-) was considered as early apoptotic cells. Higher right part (Annexin V^+/PI^+) was considered as late apoptotic cells. The results are representative of three independent experiments. (E and F) Columns represent the means ± SD values of early apoptotic and late apoptotic cells obtained from three individual experiments. $^*P < 0.05$ and $^{**}P < 0.01$ *vs.* KB or KBv200 control, respectively.

aggregates within the mitochondria, resulting in bright red staining. In apoptotic cells, due to the collapse of the membrane potential, the JC-1 cannot accumulate within the mitochondria and remains in the cytoplasm in its green-fluorescent monomeric form. As shown in Fig. 5A, 8 μM H1 treatment for 24 h led to 42.3% and 26.0% of KB and KBv200 cell membrane potential collapse, respectively.

The release of mitochondrial inter-membrane proteins into the cytosol plays a crucial role in the activation of downstream caspases, triggering DNA fragmentation and chromatin condensation. The release of mitochondrial cytochrome c and (AIF) into cytosol was detected by Western blot. As shown in Fig. 5B, cytochrome c and AIF were released into the cytosol of KB and KBv200 cells after H1 treatment for 24 h.

Mitochondrial outer membrane permeabilization (MOMP) is a decisive event in the process of cytochrome c and AIF release. Bcl-2 family proteins play a major role in the control of MOMP. To examine the association between Bcl-2 family protein expression and MOMP, the expression of anti-apoptotic protein Bcl-2 and pro-apoptotic protein Bax was determined by Western blot. As shown in Fig. 5C, H1 treatment for 24 h significantly reduced the expression of Bcl-2 and enhanced the expression of Bax. Thus, the relative ratio of Bax and Bcl-2 increased significantly. The results suggest that treatment of H1 induced apoptosis of KB and KBv200 cells was closely related to the mitochondrial pathway.

3.9. H1 increases the accumulation of ROS

Generation of ROS contributes to intrinsic apoptosis by acting an apoptotic signaling molecule. To investigate whether the ROS is involved in H1-induced apoptosis, the H_2O_2 production was determined in KB and KBv200 cells after H1 treatment. The levels

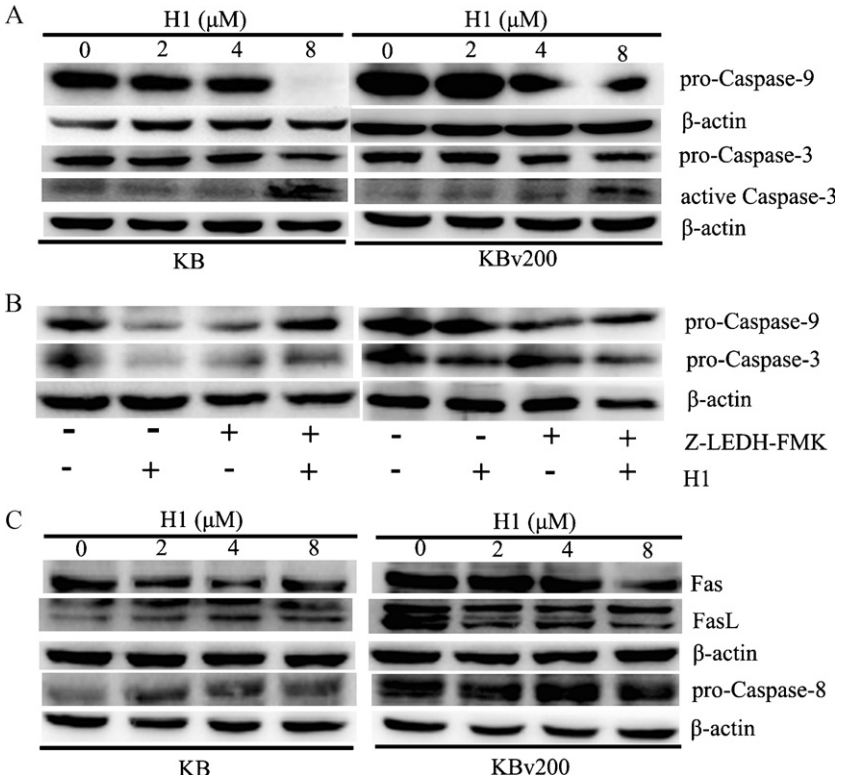

Fig. 4. H1-induced apoptosis dependent on the activation of caspase-9 and -3, but not through Fas/Fas-L mediated apoptosis. (A) Effect of H1 on the activation of caspase-9 and -3. KB and KBv200 cells treated with or without H1 for 24 h at indicated concentrations. Cells were harvested and lysed. Pro-caspase-9 and -3, cleaved active-3 were determined by Western blot analysis. (B) Cells (4×10^5/ml) were pretreated for 4 h with Z-LEDH-FMK (caspase-9 inhibitor), and exposed with or without H1 for another 24 h. Then cells were harvested and lysed. Caspase-9 and -3 in 40 μg cell lysates were detected by Western blot analysis. (C) Effect of H1 on the expression of Fas/Fas L and caspase-8 in KB and KBv200 cells. Cells were treated with or without H1 for 24 h at indicated concentrations. Cells were harvested and lysed. Fas/Fas L and caspase-8 in 40 μg cell lysates were detected by Western blot analysis. The results are representative of three individual experiments.

of ROS were increased 1.86-, 2.45-, and 3.35-folds of control in KB cells; and 1.09-, 3.34-, and 3.45-folds of control in KBv200 cells, respectively. ROS generation was significantly increased in either KB cells or KBv200 cells after cells treated by 8 μM H1. As a positive control, ROS generations significantly also increased exposure to H_2O_2, 2.45- and 3.01-fold of control in KB and KBv200 cells, respectively (Fig. 6). These results suggest that H1-induced apoptosis might be dependent of ROS generation.

3.10. H1 inhibits the activation of Erk1/2 and Akt1/2

Due to survival pathway such as Ras/Raf/Erk, PI3k/Akt/mTOR are implicated in cancer drug resistance, we detected the activation of Erk1/2 and Akt1/2 by western blot analysis. As the results shown in Fig. 7, the expression level of phosphorylated Erk1/2 and Akt 1/2 were down-regulated by H1, while the expression of Erk1/2 and Akt1/2 were not changed. Thus, the activation of Erk1/2 and Akt1/2 was suppressed by H1. It might be associated with the anti-MDR effect of H1.

4. Discussion

Failure to respond to chemotherapy represents a critical problem in the treatment of cancer [25,26]. Frequently, cancer cells exhibit resistance to one drug are accompanied by resistance to drugs whose structures and mechanisms of action may be completely different. This phenomenon is known as MDR. It is a complicated multifaceted phenomenon, and numerous signal pathways interact in cancer cells [27–30]. However, apoptosis defects and abnormal activated survival signaling pathways should be responsible to cancer drug resistance.

Recently, the development of anti-MDR agents has become a major focus on overcoming cancer drug resistance. Up to now, some compounds has been discovered with anti-MDR activity such as SB-T-12843, S9, IG105, and so on [31–33]. These agents could effectively inhibit the proliferation of cancer cells with MDR phenotype. Thus, looking for novel natural compounds and its derivatives with anti-MDR effect may be a useful strategy to circumvent MDR. Here, Our data showed that H1, a derivative of Tetradrine, led to apoptosis of both sensitive and resistant cancer cells, indicated by chromatin condensation and fragmentation of nuclei into apoptotic bodies (Fig. 4). The ability of H1-induced apoptosis is more potent than that of Tet and BrTet. Moreover, anticancer effect of H1 on resistant cancer cells xenograft is similar to that of sensitive cancer cells xenograft (Fig. 2 and Table 2). And these results demonstrated that H1 exhibited good anti-MDR activity both *in vitro* and in *vivo*.

Deficient of apoptosis is believed to contribute to cancer initiation, progression and treatment failure. It may result from inactivation of pro-apoptotic effectors, activation of anti-apoptotic factors or from reinforcement of survival pathways [34]. Previous studies showed that Tet could inhibit cell cycle progression at the G1 phase and cause apoptosis in human cancer cells [35]. Here, we detected the effect of H1 on intrinsic and extrinsic apoptosis pathway. We found apoptosis of KB and KBv200 cells induced by H1 was dependent on the activation of caspase-9 and caspase-3, but not through FasL/Fas mediated extrinsic pathway. It suggests that H1-induced apoptosis may be intrinsic apoptosis pathway-dependent.

Mitochondria are important to cell bioenergetics and play a central role in the cellular apoptosis event. Apoptosis mediated by mitochondria can trigger MOMP, which is a decisive event in the

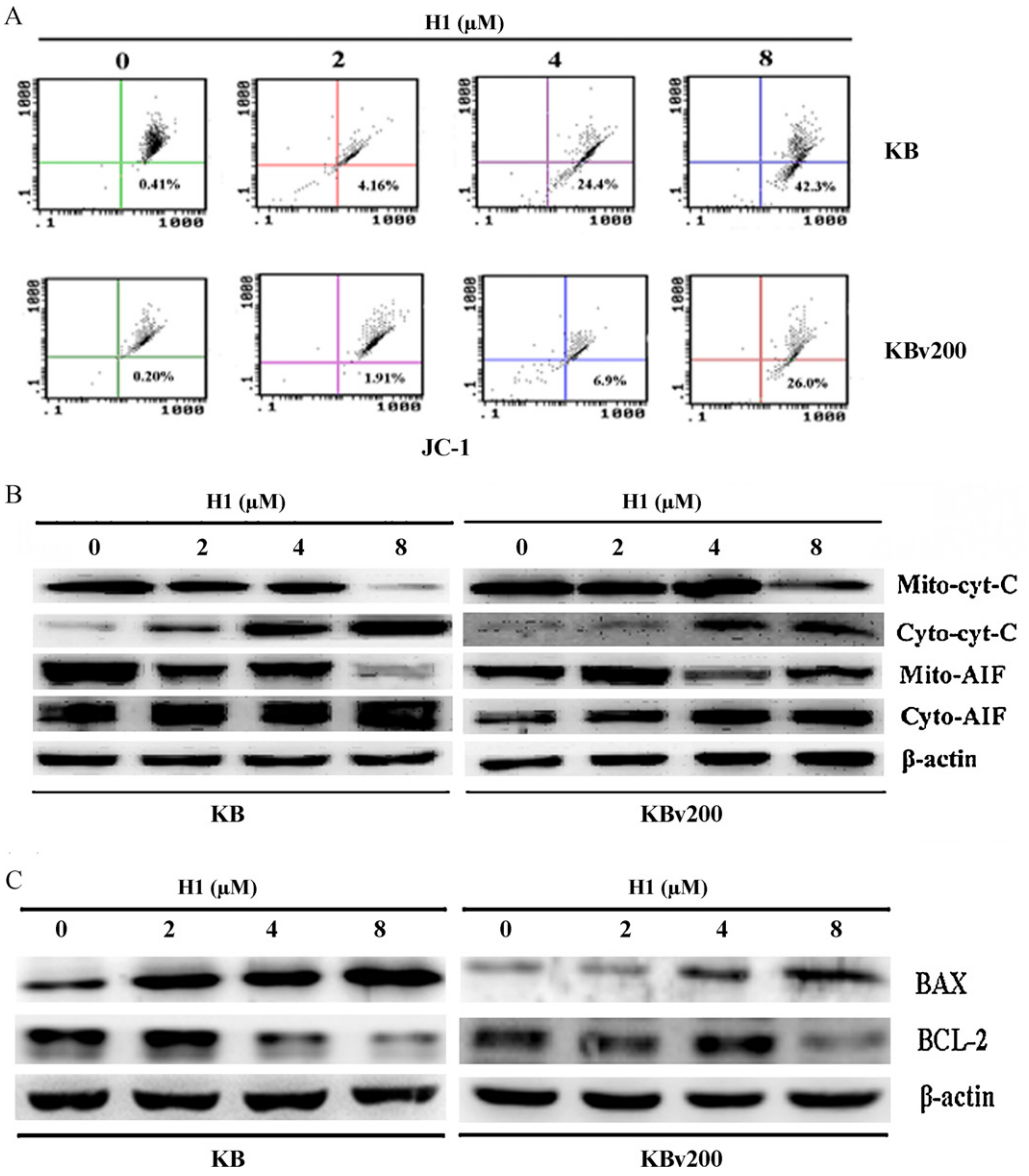

Fig. 5. H1-induced apoptosis is mediated by the mitochondrial pathway. (A) Loss mitochondrial membrane potential of cells treated by H1. KB and KBv200 cells treated with or without H1 for 24 h at indicated concentrations. The cells were harvested and washed, and then cells were incubated for 20 min in freshly prepared JC-1 solution at 37 °C. Spare dye was removed by dye buffer solution washing and cell-associated fluorescence was measured by FACS. (B) Effect of H1 on release of cytochrome c and AIF from mitochondrial to cytoplasm. KB and KBv200 cells were treated with or without H1 for 24 h at indicated concentrations. Cells were harvested and lysed, and then the mitochondrial protein and cytosol protein were prepared, respectively. The release of cytochrome c and AIF in 20 μg mitochondrial total protein and 40 μg total cytosol proteins were determined by Western blot analysis. (C) Effect of H1 on the ratio of Bax/Bcl-2 in KB and KBv200 cells. KB and KBv200 cells treated with or without H1 for 24 h at indicated concentrations. The cells were harvested and lysed. Bax and Bcl-2 in 40 μg cell lysates were detected by Western blot analysis. The results are representative of three individual experiments.

process of cytochrome c release and it has been proposed as a 'point of no return' of the mitochondrial apoptotic pathway [36]. Up to now, two nonexclusive mechanisms explaining how MOMP is induced have been proposed. The permeability transition pore complex (PTPC) plays an important role in MOMP. The PTPC is a large protein complex. Currently, it is believed that the major PTPC components are the voltage-dependent anion channel, an outer mitochondrial membrane protein, the adenine nucleotide translocator (ANT) in inner mitochondrial membrane, cyclophilin D (CypD) in the matrix and the mitochondrial benzodiazepine receptor (PBR) [37]. Many stimuli such as increased cytosolic Ca^{2+} or reaction oxygen species (ROS) promote the PTPC opening. As the PTPC opens, low molecular weight solutes and water enter to cause the loss in $\Delta\Psi_m$, mitochondrial matrix swelling and rupturing of the outer mitochondrial membrane. Mitochondrial damage results from permeabilization of the outermitochondrial membrane which facilitates cytochrome c release into the cytoplasm [38]. Our data showed that H1 led to increase of ROS generation, loss of $\Delta\Psi_m$, and the release of cytochrome c from mitochondria also increased in both KB and KBv200 cells (Fig. 6).

Moreover, MOMP can be regulated by Bcl-2 family, which consists of more than 20 members of pro-apoptotic proteins (including Bax, Bak, Bad, Bid, Bik, and so on), and anti-apoptotic proteins (including Bcl-2, Bcl-XL, Mcl-1, and so on). Members of the Bcl-2 family can form homo- or hetero-dimers, thereby functioning as agonists or antagonists of each other. Pro-apoptotic members of the Bcl-2 family such as Bax, Bak, Bim, induce the release of cytochrome c from mitochondria, whereas anti-apoptotic members such as Bcl-XL can bind and inactivate Apaf-1 [39]. Importantly, changes the ratio of pro-apoptosis Bcl-2 protein and anti-apoptosis Bcl-2 protein refer to chemotherapy resistance in many cancers [40]. Tet could induce cleavage of

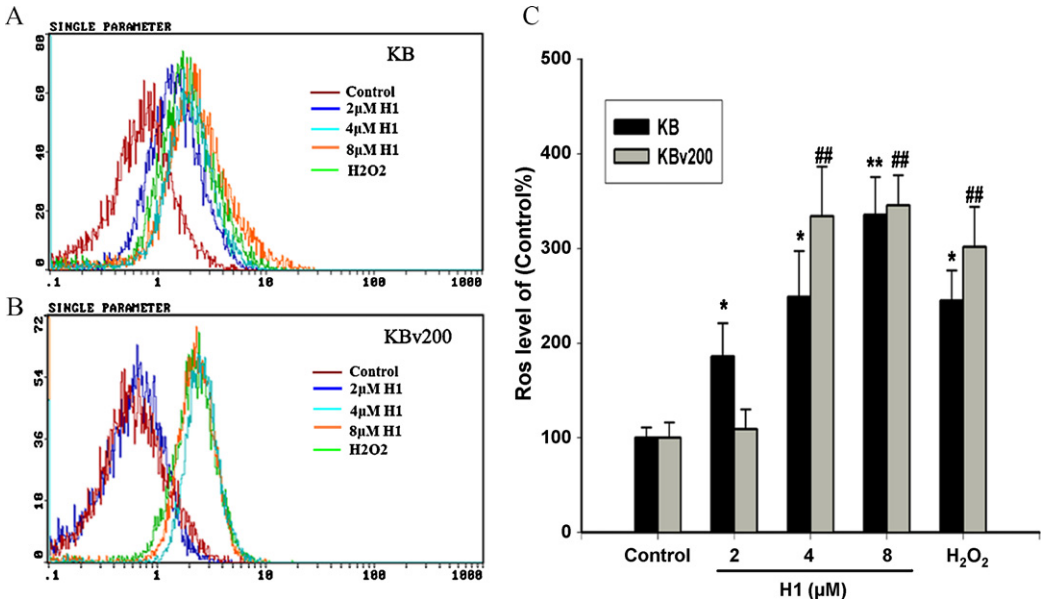

Fig. 6. H1 increased the generation of ROS in KB cells and KBv200 cells. After cells treated with desired concentrations of H1 for 24 h, ROS production was determined by flow cytometry. ROS levels treated with H_2O_2 were higher than the control in both cell lines. Significant increases of ROS production were observed at 4 μM of H1 in KB and KBv200 cells. (A) and (B) represented the histogram of ROS production in KB and KBv200 cells, respectively. The results are representative of three individual experiments. (C) Columns represent the means ± SD values obtained from three individual experiments. $^{**}P < 0.01$, *vs.* KB control; $^{\#}P < 0.05$, $^{\#\#}P < 0.01$ *vs.* KBv200 control, respectively.

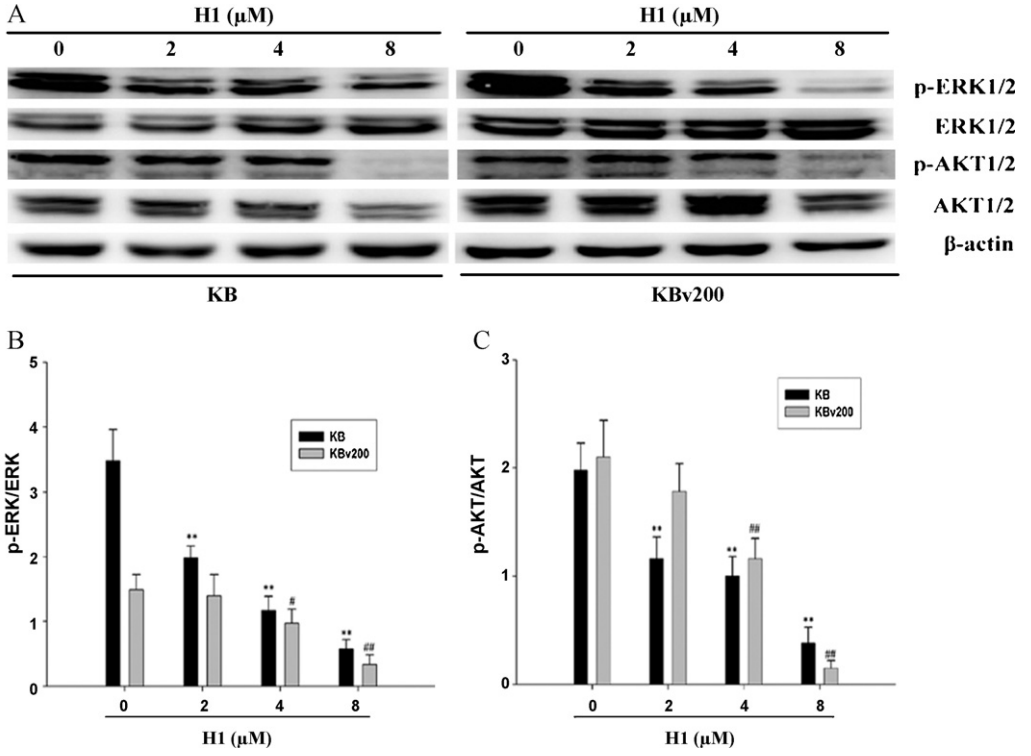

Fig. 7. H1 inhibited the activation of Erk1/2 and Akt1/2. KB and KBv200 cells were treated with or without H1 for 24 h at indicated concentrations. Then cells were harvested and lysed. Erk1/2 and Akt1/2, phosphate-Erk1/2 and phosphate-Akt1/2 in 40 μg cell lysates were detected by Western blot analysis. Columns represent the means ± SD values obtained from three individual experiments. $^{**}P < 0.01$, *vs.* KB control; $^{\#}P < 0.05$, $^{\#\#}P < 0.01$ *vs.* KBv200 control, respectively. The results are representative of three individual experiments.

Bid and downregulate Bcl-XL in human hepatoblastoma cells [41]. It also found significant correlation between sensitivity to Tet and cellular expression of Bcl-2 [42]. In addition, our previous studies showed that BrTet could enhance the sensitivity of Bel7402 cells to Dox, and its mechanisms were associated with the elevation of Bax/Bcl-2 ratio [43]. Here, we determined the ratio of Bax/Bcl-2 in both sensitive and resistant cells which treated by H1. Our data showed that H1 up-regulated the expression of Bax, and down-regulated the expression of Bcl-2. Thus, the ratio of Bax and Bcl-2 increased significantly. Therefore, the alteration of the ratio of pro-apoptotic and anti-apoptotic Bcl-2 family members may be another important mechanism for the effect of H1 on apoptosis of KB and KBv200 cells.

Raf/Raf/Erk and PI3K/Akt/mTOR pathways are invariably implicated in cancer drug resistance. In certain cancer types, Ras/Raf/Erk pathway could modulate anti-apoptotic molecules expression such as Bcl-2 [44]. This increased expression of Bcl-2 most likely occurs by a transcriptional mechanism by downstream target kinases of the Raf/Raf/Erk pathway inducing the phosphorylation of transcription factors which bind the promoter regions of Bcl-2 and stimulate transcription. PI3K/Akt/mTOR pathway has been related to increase drug resistance in many tumors. Loss of regulation of PI3K results in increasing activity of Akt, which exerts multiple anti-apoptotic functions. For example, phosphorylation of Bax, Bad and caspase-9 [45] as well as inactivation of pro-apoptotic transcription factors such as FoxO and p53 [46]. It has reported that Tet could inhibit the activation of Akt in human colon cancer cells and human hepatocellular carcinoma [47], and suppress the activation of Erk in human lung cancer [48]. Based on these findings, we determined the effect of H1 on the activation of Erk1/2 and Akt1/2. Our results showed that H1 could inhibit the activation of Erk1/2 and Akt1/2 with good concentration-dependent manner (Fig. 7).

In conclusion, H1 exerted good anti-MDR activity both *in vitro* and *in vivo*. It did not affect the cell cycle distribution and induced apoptosis in both KB and KBv200 cells. Further studies showed that its mechanisms may be implicated in initiating intrinsic apoptosis pathway and inhibiting the activation of Erk1/2 and Akt1/2. These findings further support the potential of H1 to be used in clinical trial of MDR cancer treatment.

Acknowledgements

We would like to dedicate this manuscript to the memory of Academician Geng-Tao Liu, who unfortunately passed away during the preparation of this manuscript.

This work was supported by Grants (No. 30630069) from China National Natural Sciences Foundation.

References

[1] Miao ZH, Ding J. Research advances on circumventing tumor multidrug resistance. Ai Zheng 2003;22:886–92.
[2] Shabbits JA, Hu Y, Mayer LD. Tumor chemosensitization strategies based on apoptosis manipulations. Mol Cancer Ther 2003;2:805–13.
[3] Szakacs G, Paterson JK, Ludwig JA, Booth-Genthe C, Gottesman MM. Targeting multidrug resistance in cancer. Nat Rev Drug Discov 2006;5:219–34.
[4] Mimeault M, Hauke R, Batra SK. Recent advances on the molecular mechanisms involved in the drug resistance of cancer cells and novel targeting therapies. Clin Pharmacol Ther 2008;83:673–91.
[5] Fadeel B, Orrenius S, Apoptosis:. a basic biological phenomenon with wide-ranging implications in human disease. J Intern Med 2005;258:479–517.
[6] Green DR, Kroemer G. Pharmacological manipulation of cell death: clinical applications in sight? J Clin Invest 2005;115:2610–7.
[7] Krammer PH. CD95(APO-1/Fas)-mediated apoptosis: live and let die. Adv Immunol 1999;71:163–210.
[8] Li-Weber M, Krammer PH. Function and regulation of the CD95 (APO-1/Fas) ligand in the immune system. Semin Immunol 2003;15:145–57.
[9] Fulda S, Kufer MU, Meyer E, van Valen F, Dockhorn-Dworniczak B, Debatin KM. Sensitization for death receptor- or drug-induced apoptosis by re-expression of caspase-8 through demethylation or gene transfer. Oncogene 2001;20:5865–77.
[10] Jiang CC, Chen LH, Gillespie S, Kiejda KA, Mhaidat N, Wang YF, et al. Tunicamycin sensitizes human melanoma cells to tumor necrosis factor-related apoptosis-inducing ligand-induced apoptosis by up-regulation of TRAIL-R2 via the unfolded protein response. Cancer Res 2007;67:5880–8.
[11] Wagner KW, Punnoose EA, Januario T, Lawrence DA, Pitti RM, Lancaster K, et al. Death-receptor O-glycosylation controls tumor-cell sensitivity to the proapoptotic ligand Apo2L/TRAIL. Nat Med 2007;13:1070–7.
[12] Martelli AM, Evangelisti C, Chiarini F, Grimaldi C, Manzoli L, McCubrey JA. Targeting the PI3K/AKT/mTOR signaling network in acute myelogenous leukemia. Expert Opin Investig Drugs 2009;18:1333–49.
[13] Siddik ZH. Cisplat mode of cytotoxic action molecular basis of resistance. Oncogene 2003;22:7265–79.
[14] Kawauchi K, Ogasawara T, Yasuyama M, Otsuka K, Yamada O. Regulation and importance of the PI3K/Akt/mTOR signaling pathway in hematologic malignancies. Anti-Cancer Agents Med Chem 2009;9:1024–38.
[15] Zhao Y, You H, Yang Y, Wei L, Zhang X, Yao L, et al. Distinctive regulation and function of PI 3K/Akt and MAPKs in doxorubicin-induced apoptosis of human lung adenocarcinoma cells. J Cell Biochem 2004;91:621–32.
[16] Wu JM, Chen Y, Chen JC, Lin TY, Tseng SH. Tetrandrine induces apoptosis and growth suppression of colon cancer cells in mice. Cancer Lett 2010;287:187–95.
[17] Chen Y, Chen JC, Tseng SH. Tetrandrine suppresses tumor growth and angiogenesis of gliomas in rats. Int J Cancer 2009;124:2260–9.
[18] Wang G, Lemos JR, Iadecola C. Herbal alkaloid tetrandrine: fron an ion channel blocker to inhibitor of tumor proliferation. Trends Pharmacol Sci 2004;25:120–3.
[19] Kuo PL, Lin CC. Tetrandrine-induced cell cycle arrest and apoptosis in Hep G2 cells. Life Sci 2003;73:243–52.
[20] Jin J, Wang FP, Wei H, Liu G. Reversal of multidrug resistance of cancer through inhibition of P-glycoprotein by 5-bromotetrandrine. Cancer Chemother Pharmacol 2005;55:179–88.
[21] Wei N, Sun H, Wang F, Liu G. H1, a novel derivative of tetrandrine reverse P-glycoprotein-mediated multidrug resistance by inhibiting transport function and expression of P-glycoprotein. Cancer Chemother Pharmacol 2011;67:1017–25.
[22] Shi Z, Tiwari AK, Shukla S, Robey RW, Kim IW, Parmar S, et al. Inhibiting the function of ABCB1 and ABCG2 by the EGFR tyrosine kinase inhibitor AG1478. Biochem Pharmacol 2009;77:781–93.
[23] Lin S, Fujii M, Hou DX. Rhein induces apoptosis in HL-60 cells via reactive oxygen species-independent mitochondrial death pathway. Arch Biochem Biophys 2003;418:99–107.
[24] Alley MC, Hollingshead MG, Dykes DJ, Waud WR. Human tumor xenograft models in NCI drug development. In: Teicher BA, Andrews PA, editors. Anticancer drug development guide. Totowa, NJ: Humana Press; 2004 p. 125–52.
[25] Liscovitch M, Lavie Y. Cancer multidrug resistance: a review of recent drug discovery research. IDrugs 2002;5:349–55.
[26] Wei N, Sun H, Liu GT. Advances in the targeting ATP-binding cassette transporters to overcome tumor multi-drug resistance. Acta Pharm Sin 2010;45:1205–11.
[27] McCubrey JA, Steelman LS, Chappell WH, Abrams SL, Wong EW, Chang F, et al. Roles of the Raf/MEK/ERK pathway in cell growth, malignant transformation and drug resistance. Biochim Biophys Acta 2007;1773:1263–84.
[28] Zhang Z, Wu JY, Hait WN, Yang JM. Regulation of the stability of P-glycoprotein by ubiquitination. Mol Pharmacol 2004;66:395–403.
[29] Deininger M. Resistance and relapse with imatinib in CML: causes and consequences. J Natl Compr Cancer Netw 2008;6(Suppl. 2):S11–21.
[30] Alaoui-Jamali MA, Qiang H. The interface between ErbB and non-ErbB receptors in tumor invasion: clinical implications and opportunities for target discovery. Drug Resist Updat 2003;6:95–107.
[31] Ojima I, Slater JC, Michaud E, Kuduk SD, Bounaud PY, Vrignaud P, et al. Syntheses and structure–activity relationships of the second-generation antitumor taxoids: exceptional activity against drug-resistant cancer cells. J Med Chem 1996;39:3889–96.
[32] Zhang C, Yang N, Yang CH, Ding HS, Luo C, Zhang Y, et al. S9, a novel anticancer agent, exerts its anti-proliferative activity by interfering with both PI3K-Akt-mTOR signaling and microtubule cytoskeleton. PLoS ONE 2009;4:e4881.
[33] Wang YM, Hu LX, Liu ZM, You XF, Zhang SH, Qu JR, et al. N-(2,6-dimethoxypyridine-3-yl)-9-methylcarbazole-3-sulfonamide as a novel tubulin ligand against human cancer. Clin Cancer Res 2008;14:6218–27.
[34] Ma Y, Ding Z, Qian Y, Shi X, Castranova V, Harner EJ, et al. Predicting cancer drug response by proteomic profiling. Clin Cancer Res 2006;12:4583–9.
[35] Meng LH, Zhang H, Hayward L, Takemura H, Shao RG, Pommier Y. Tetrandrine induces early G1 arrest in human colon carcinoma cells by down-regulating the activity and inducing the degradation of G1-S-specific cyclin-dependent kinases and by inducing p53 and p21Cip1. Cancer Res 2004;64:9086–92.
[36] Fesik SW, Shi Y, Structural biology. Controlling the caspases. Science 2001;294:1477–8.
[37] Mattson MP, Chan SL. Calcium orchestrates apoptosis. Nat Cell Biol 2003;5:1041–3.
[38] Dejean LM, Martinez-Caballero S, Kinnally KW. Is MAC the knife that cuts cytochrome c from mitochondria during apoptosis? Cell Death Differ 2006;13:1387–95.
[39] Dejean LM, Ryu SY, Martinez-Caballero S, Teijido O, Peixoto PM, Kinnally KW. MAC and Bcl-2 family proteins conspire in a deadly plot. Biochim Biophys Acta 2010;1797:1231–8.
[40] Dejean LM, Martinez-Caballero S, Manon S, Kinnally KW. Regulation of the mitochondrial apoptosis-induced channel, MAC, by BCL-2 family proteins. Biochim Biophys Acta 2006;1762:191–201.
[41] Oh SH, Lee BH. Induction of apoptosis in human hepatoblastoma cells by tetrandrine via caspase-dependent Bid cleavage and cytochrome c release. Biochem Pharmacol 2003;66:725–31.
[42] Cho HS, Chang SH, Chung YS, Shin JY, Park SJ, Lee ES, et al. Synergistic effect of ERK inhibition on tetrandrine-induced apoptosis in A549 human lung carcinoma cells. J Vet Sci 2009;10:23–8.
[43] Liu XD, Sun H, Liu GT. 5-Bromotetrandrine enhances the sensitivity of doxorubicin-induced apoptosis in intrinsic resistant human hepatic cancer Bel7402 cells Cancer letters 2010;292:24–31.
[44] Mizuno R, Oya M, Hara S, Matsumoto M, Horiguchi A, Ohigashi T, et al. Modulation of bcl-2 family proteins in MAPK independent apoptosis induced

by a cdc25 phosphatase inhibitor Cpd 5 in renal cancer cells. Oncol Rep 2005;14:639–44.
[45] Gardai SJ, Hildeman DA, Frankel SK, Whitlock BB, Frasch SC, Borregaard N, et al. Phosphorylation of Bax Ser184 by Akt regulates its activity and apoptosis in neutrophils. J Biol Chem 2004;279:21085–9.
[46] Manning BD, Cantley LC. AKT/PKB signaling: navigating downstream. Cell 2007;129:1261–74.
[47] Liu C, Gong K, Mao X, Li W. Tetrandrine induces apoptosis by activating reactive oxygen species and repressing Akt activity in human hepatocellular carcinoma. Int J Cancer 2011;129:1519–31.
[48] Liu B, Wang T, Qian X, Liu G, Yu L, Ding Y. Anticancer effect of tetrandrine on primary cancer cells isolated from ascites and pleural fluids. Cancer Lett 2008;268:166–75.